Final Technical Report

on

INVESTIGATION OF INFRA-RED AND NONEQUILIBRIUM AIR RADIATION

Grant No. NAG 2-910

Prepared for

NATIONAL AERONAUTICS AND SPACE ADMINISTRATION

For the Period

May 1, 1994 to October 31, 1996

Submitted by

Charles H. Kruger, Principal Investigator
Christophe O. Laux, Associate Investigator
High Temperature Gasdynamics Laboratory
Mechanical Engineering Department
Stanford University
Stanford, California 94305-3032

HIGH TEMPERATURE GASDYNAMICS LABORATORY
Mechanical Engineering Department
Stanford University

HTGL

Final Technical Report

on

INVESTIGATION OF INFRA-RED AND NONEQUILIBRIUM AIR RADIATION

Grant No. NAG 2-910

Prepared for

NATIONAL AERONAUTICS AND SPACE ADMINISTRATION

For the Period

May 1, 1994 to October 31, 1996

Submitted by

C.H. Kruger, Principal Investigator
C. O. Laux, Associate Investigator
High Temperature Gasdynamics Laboratory
Mechanical Engineering Department
Stanford University
Stanford, California 94305-3032

Contents

1. Abstract

This report summarizes the results obtained during a research program on the infrared radiation of air plasmas conducted in the High Temperature Gasdynamics Laboratory at Stanford University. This research was supported by a grant from the National Aeronautics and Space Administration (NAG 2-910), under the direction of Professor Charles H. Kruger, with Dr. Stephen R. Langhoff from NASA-Ames as technical monitor.

This program was intended to investigate the masking of infrared signatures by the air plasma formed behind the bow shock of high velocity missiles. Prior to this work, the radiative emission of air plasmas in the infrared had been the object of few experimental investigations, and although several infrared systems were already modeled in radiation codes such as NEQAIR, measurements were required to validate numerical predictions and indicate whether all transitions of importance were accounted for in the model. The program was further motivated by the fact that 9 excited states (A, B, C, D, B', F, H, and H') of NO radiate in the infrared, especially between 1 and 1.5 μm where at least 9 transitions involving can be observed. Because these IR transitions are relatively well separated from each other, excited NO states concentrations can be easily measured, thus providing essential information on excited-state chemistry for use in optical diagnostics or in electronic excitation model validation. Developing accurate collisional-radiative models for these excited NO states is of importance as the UV-VUV transitions of NO (beta, gamma, delta, epsilon, beta prime, gamma prime) produce a major, if not dominant, fraction of the radiation emitted by air plasmas.

Accurate measurements were made of the spectral emission of air plasmas in the infrared between 0.8 and 5.5 μm. A 50 kW radio-frequency inductively-coupled plasma torch was used to produce atmospheric pressure air in local thermodynamic equilibrium with temperatures up to ~ 7900 K. The absolute intensity of the measured spectral emission is estimated to be better than 10%. These experimental spectra were used as benchmarks to guide the extension of the radiation code NEQAIR into the infrared spectral range. In addition to the radiating systems of the baseline NEQAIR (N_2 first positive and CN red systems, atomic nitrogen and oxygen lines, free-bound, and free-free continua), the extended code, called NEQAIR2-IR, now includes eight electronic NO transitions, the vibrational-rotational band systems of NO and CO, the Meinel system of N_2^+ and 360 additional lines of atomic oxygen and nitrogen. Detailed comparisons between measured and simulated spectra are presented.

2. Research Accomplishments

2.1 Introduction

In-flight detection of infrared signatures is partly limited to spectral windows of atmospheric transmission (Fig. 1), but also to spectral ranges where the air plasma behind the bow-shock of the detector-carrying vehicle is sufficiently transparent. While atmospheric windows are well documented,[1,2] the radiation of air plasmas in the infrared has been the object of few experimental investigations. And although some infrared systems are presently modeled in high-temperature radiation codes such as NEQAIR,[3] spectral measurements are required to validate numerical predictions and determine whether all intense transitions are taken into account. Accurate, detailed models of infrared air radiation are also important for optical diagnostics as temperature and concentration measurements can be made using the numerous atomic and molecular transitions that appear in the infrared (vibration-rotation spectrum of ground state NO, electronic transitions between excited NO states, the free-free and free-bound atomic recombination continua, atomic oxygen and nitrogen lines, and electronic systems of N_2 and N_2^+). Of particular interest are electronic transitions of NO in the range 0.9-1.3 μm which can be used to measure the concentrations of several excited NO states, including the A, C, D, E, F, H, and H' states. Measurements of these concentrations in nonequilibrium plasmas would provide data to test nonequilibrium re-entry radiation codes[3] as the UV-VUV transitions of NO (gamma, delta, epsilon,...) that issue from the same excited states produce a major, if not dominant, fraction of the radiation emitted by air plasmas.[4] Unlike the UV-VUV systems which overlap so much that excited state populations can only be extracted by very high resolution measurements, the infrared electronic systems of NO are relatively well separated from each other and thus easier to measure.

The goals of the present work were a) identify experimentally the radiating systems of importance in the range 0.8 to 5.5 μm, b) build a state-of-the-art model for infrared high-temperature air radiation, and c) establish for which radiating systems additional data, such as accurate transition probabilities and term energies, are needed to improve the model.

In this report, we first present our measurements of high-temperature air emission in the spectral range 0.8-5.5 μm. A 50 kW radio-frequency (RF) induction plasma torch was used to produce a steady-state flowing atmospheric pressure plasma at temperatures approaching 8000 K. In previous works at similar operating conditions,[5] the thermodynamic state of the plasma had been shown to be close to local thermodynamic equilibrium. Furthermore, spatial profiles of temperature and species concentrations had been accurately determined. The measured emission spectra can be compared with the

predictions of an equilibrium radiation model, thus avoiding the complications associated with nonequilibrium populations in the emitting levels. In the second part of this report, we describe how these measurements were used as benchmarks to guide the development of an infrared radiation model built on the basis of NEQAIR2.[6,7] For sake of clarity, the extended infrared radiation code is hereafter termed NEQAIR2-IR. After a brief description of the plasma torch facility and the experimental setup, a detailed analysis is presented of the experimental and modeling results obtained between 0.8 and 5.5 μm.

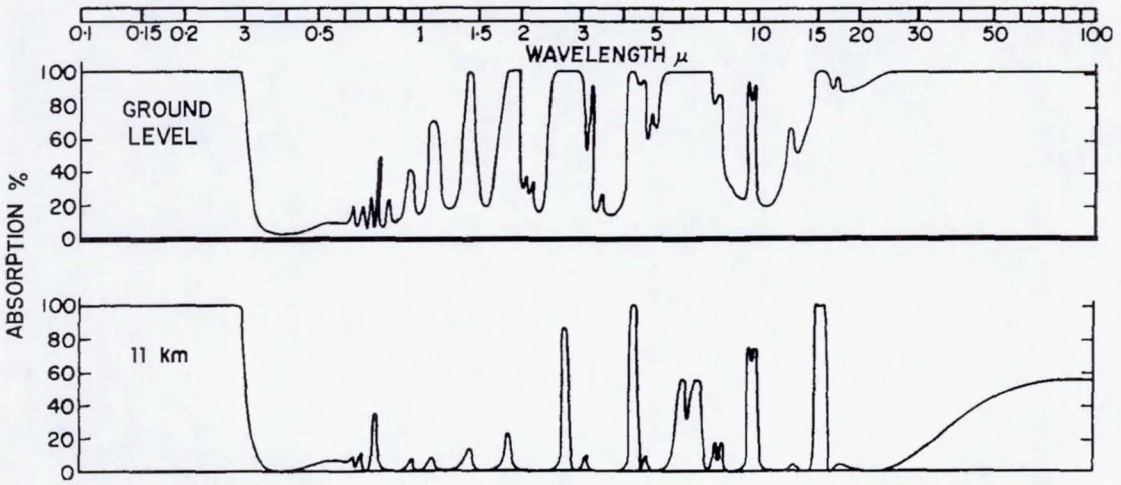

Figure 1. Atmospheric absorption spectrum for a solar beam reaching ground level (top curve). The same for a beam reaching an altitude of 11 km (bottom curve). Excerpted from Ref. [1].

2.2 Experimental Set-Up

The experimental work was conducted in a 50 kW TAFA model 66 RF induction plasma torch powered by a LEPEL model T-50-3 power supply operating at a frequency of 4 MHz. A copper nozzle of 5.0 cm exit diameter was utilized at the top of the upward firing torch. All measurements were made 1 cm downstream of the nozzle exit in a region where the flow is laminar. As shown in Fig. 2, the set-up for spectral measurements includes a SPEX model 750M 3/4 meter scanning monochromator fitted with a Cincinnati Electronics model SDD-20E1-S1 indium-antimonide cryogenically-cooled (liquid N_2) infrared detector with integrated pre-amplifier. A 1200 grooves/mm grating blazed at 0.5 μm was used for temperature measurements from the atomic oxygen triplet transition at 0.7774 μm and for spectral emission measurements between 0.8 and 1.1 μm. A 600 gr/mm grating blazed at 2.0 μm was used for spectral measurements between 1.0 and 3.0 μm, and a 300 gr/mm grating blazed at 4.0 μm between 3.0 and 6.0 μm. High-order interferences were rejected by using appropriate long-pass filters with cut-offs at 0.4, 0.8, 1.5 and 3.0 μm. Various combinations of monochromator slit width settings, gratings and filters were used to cover the spectral range 0.8 to 5.5 μm. Table 1 summarizes these arrangements.

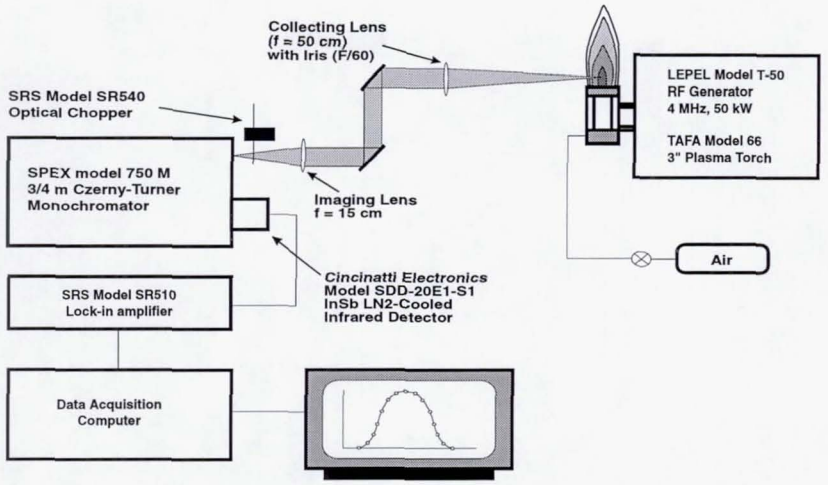

Figure 2. Set-up for spectral emission measurements.

The collecting and imaging lenses were made of calcium fluoride, a material chosen for its excellent transmissivity (greater than 90%) in the spectral range of interest. Data were acquired with a Stanford Research Systems model SR510 lock-in amplifier (later upgraded with a Stanford Research Systems model SR830 lock-in amplifier) and then transferred and stored on a laboratory computer for processing. Absolute calibrations of the experimental spectra were performed with an Optronics model OL550 tungsten strip lamp of spectral radiance traceable to NIST standards in the range 0.25–6.0 μm.

Table 1. Scheme for measurements in range 0.8-5.5 μm.

Spectral range (μm)	Blaze wavelength λ (μm)	Groove density (gr/mm)	Filter cut-off λ_{min} (μm)	Slit widths[a] (mm)
0.8-1.1	0.5	1200	0.8	0.70/2.00
1.0-1.5	2.0	600	0.8	0.35/1.00
1.5-3.0	2.0	600	1.5	0.35/1.00
3.0-5.5	4.0	300	3.0	0.50/2.00

a) Entrance slit/exit slit.

The spectral resolution in the various ranges is determined by the slit function which, for entrance and exit slits of width w_1 and w_2, is well approximated by a trapezoid of base and top:

$$\Delta\lambda_{base} = (w_1 + w_2)\frac{d\lambda}{dx} \tag{1a}$$

$$\Delta\lambda_{top} = |w_2 - w_1|\frac{d\lambda}{dx}. \tag{1b}$$

In Eqn. (1), the quantity $d\lambda/dx$ stands for the reciprocal linear dispersion of the instrument (typically in units of Å/mm). For monochromators of the Czerny-Turner type (such as the SPEX 750M used here), the reciprocal linear dispersion is given by the following equation which can be derived from the fundamental grating equation and from trigonometric relations:

$$\frac{d\lambda}{dx} = \frac{\lambda}{2f}\left(\tan\Phi + \sqrt{\left(\frac{2d}{m\lambda}\cos\Phi\right)^2 - 1}\right). \tag{2}$$

In the above expression, f represents the focal length of the monochromator, d the spacing between the grooves of the grating, m the order of dispersion, and Φ (equal to ~6.86° for the SPEX 750M) is half the angle between the lines joining the center of the grating to the centers of the two mirrors of the monochromator. All measurements here were made in first order (m = 1) and the monochromator focal length was 0.75 m. Shown in Fig. 3 are the reciprocal linear dispersion curves of the three gratings. These wavelength-dependent dispersions were taken into account both in the experimental calibration and in the simulations. It should be noted that ignoring the variations of the linear dispersion with wavelength would have resulted in large errors (by up to a factor 2) for the present experiments.

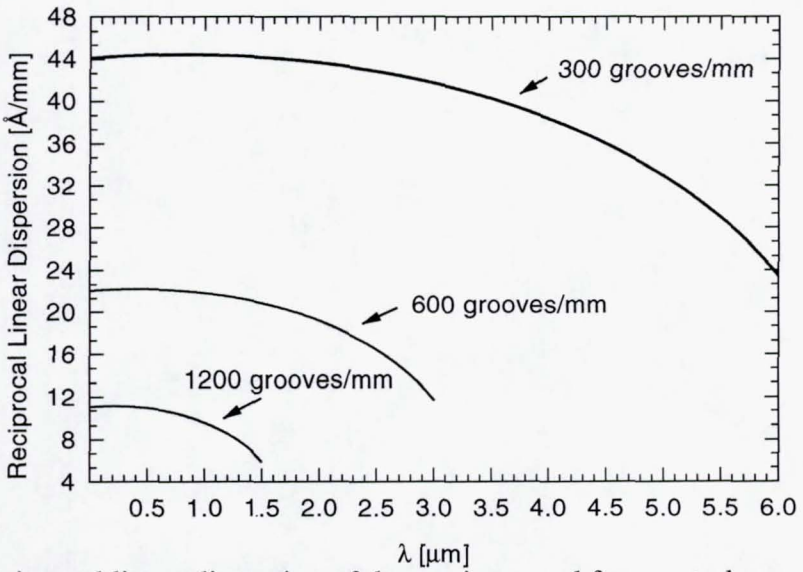

Figure 3. Reciprocal linear dispersion of the gratings used for spectral measurements.

2.3 Thermodynamic State of the Plasma

The plasma torch was operated here at conditions similar to those of earlier studies[5] wherein measurements of electronic, vibrational, and rotational temperatures, along with electron number densities, had shown that the plasma was close to local thermodynamic equilibrium, i.e. chemical and thermal equilibrium. In these earlier studies, it was also shown that the radial temperature profile of the plasma could be determined most accurately (within ~1%) by measuring and Abel-inverting lateral absolute intensity profiles of the atomic oxygen transition at 7774 Å. Figure 4 shows the measured temperature profile corresponding to the conditions of the present work. (This profile was measured out to a radius of 1.9 cm; beyond this radial location, the intensity of the O line radiation was too weak to be detected). Since the plasma is close to LTE, species concentrations can be calculated assuming chemical equilibrium, and the populations of all internal energy states can be determined by assuming Boltzmann distributions at a single temperature. These quantities can then be used to simulate numerically the measured line-of-sight spectra.

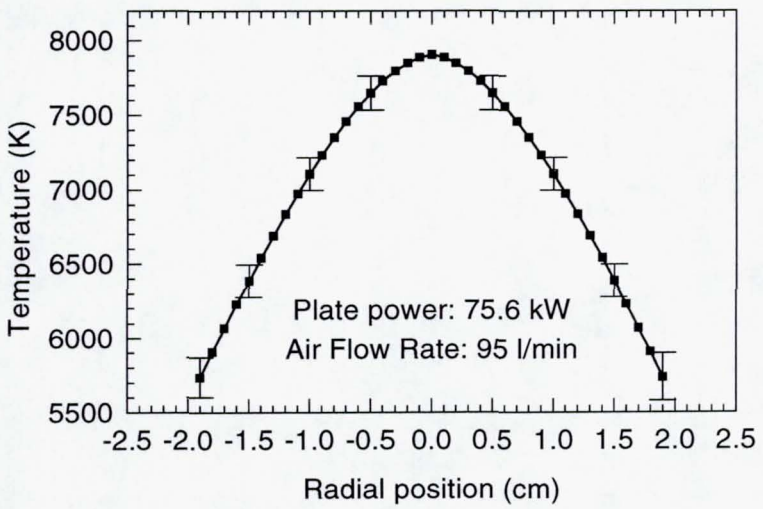

Figure 4. Measured LTE temperature profile.

2.4 Spectral Measurements

In the following sections, the emission spectra measured along the plasma diameter between 0.8 and 5.5 μm are presented. As mentioned earlier, these spectra were corrected for the spectral response of the detection system and calibrated in intensity. The accuracy of the spectral intensities is estimated to be better than 10% over the whole spectral range. Numerical simulations were conducted by dividing the plasma into 50 slabs of 1-mm thickness in which the concentrations and temperature were assumed uniform and given by the measured temperature profile. The baseline NEQAIR model included a limited number of infrared transitions: N_2 first positive, CN red, atomic oxygen and nitrogen lines between 0.8 and 1.3 μm, and the free-free and bound-free continua of atomic oxygen and nitrogen. As will be seen in subsequent sections, the measured spectra exhibit numerous spectral features due to transitions not modeled in the baseline NEQAIR2. Many of these structures were identified and incorporated into NEQAIR2-IR.

2.4.1 Range 0.8–1.5 μm

In the experimental spectra measured over this range, the most intense features are atomic lines of oxygen and nitrogen. As can be seen in Figs. 5 and 6, the baseline NEQAIR2 model reproduces these lines accurately, but some structure between the lines is missing. Previous investigations conducted by Wray[8] in an atmospheric pressure arcjet had shown that these features correspond to electronic transitions between high-lying Rydberg states of NO. The NO systems listed in Table 2 were then incorporated into NEQAIR2-IR as detailed below.

Table 2. Infrared electronic transitions of NO. Band origins and absorption band oscillator strengths.

Electronic Transition	v′–v″	Band Origin (μm)	Oscillator Strength	Source
$C\ ^2\Pi - A\ ^2\Sigma^+$	0-0	1.22	0.465	(a)
	1-1	1.22	0.464	
$D\ ^2\Sigma^+ - A\ ^2\Sigma^+$	0-0	1.10	0.258	Sheehy et al.[9]
	1-1	1.11	0.256	
$E\ ^2\Sigma^+ - C\ ^2\Pi$	0-0	1.18	< 0.06	Wray[8] (b)
$H'\ ^2\Pi - C\ ^2\Pi$	or	0.97	0.15	
$H\ ^2\Sigma^+ - D\ ^2\Sigma^+$	1-1	1.06	0.25	
$H'\ ^2\Pi - D\ ^2\Sigma^+$		1.06	0.25	
$E\ ^2\Sigma^+ - D\ ^2\Sigma^+$	0-0	1.321	0.75	(c)
$F\ ^2\Delta - C\ ^2\Pi$	0-0	1.033	0.44	(d)
$H\ ^2\Sigma^+ - C\ ^2\Pi$	0-0	0.968	0.48	(d)

(a) Based on the ETMF computed by Sheehy et al[9] for the D–A transition (see text for justification).
(b) Ref. 8 lists emission band oscillator strengths; in this table, they are converted to absorption strengths.
(c) As no previous measurements exist, this value was obtained by matching the measured spectrum
(d) Twice the value measured by Wray.[8]

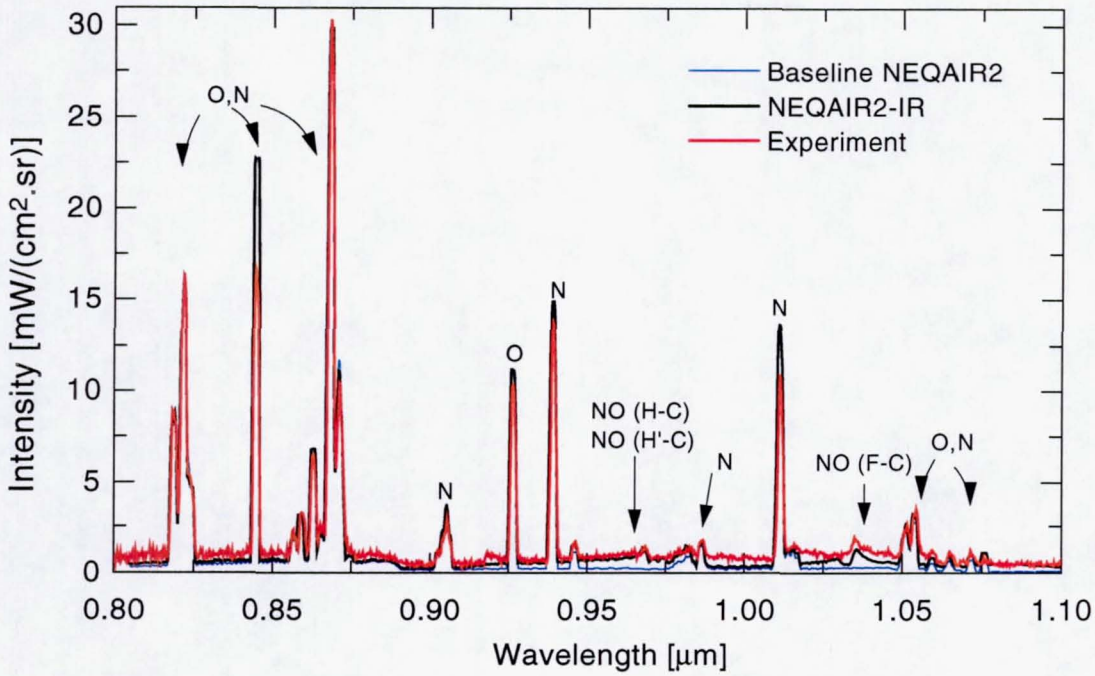

Figure 5. Comparison between the measured spectrum, baseline NEQAIR2 model (includes only O and N lines and the first positive system of N_2), and NEQAIR2-IR: 0.8 – 1.1 μm.

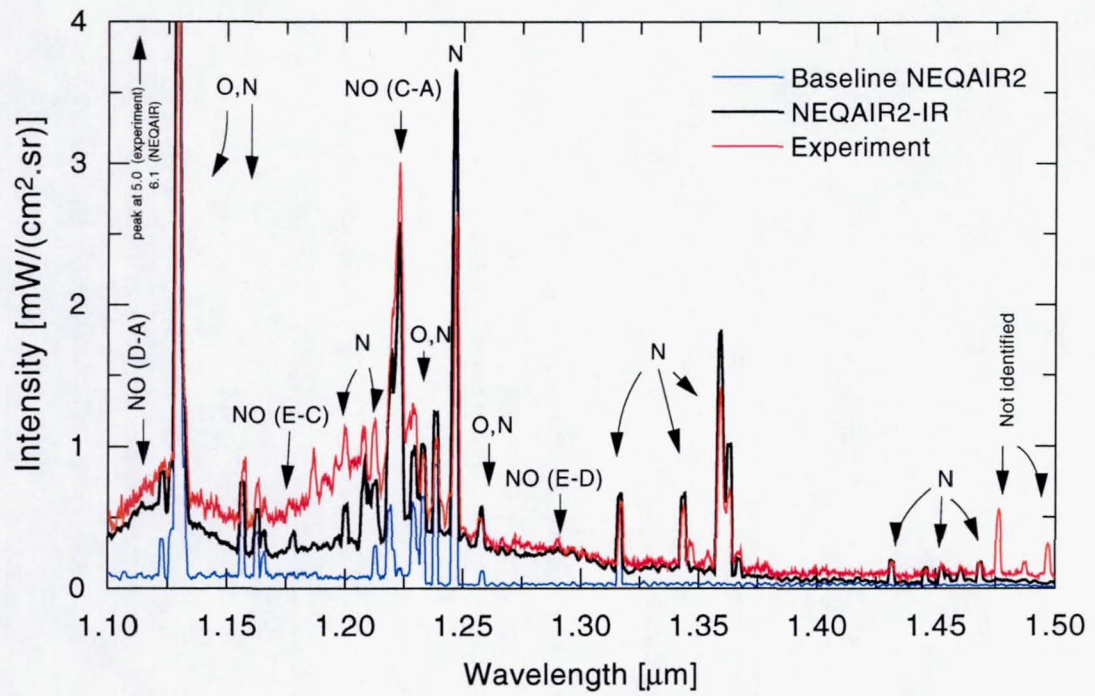

Figure 6. Measurements and simulations: 1.0 – 1.5 μm.

For the D-A band system (also called the "11,000 Å" system), transition probabilities were calculated using the accurate electronic transition moment function (ETMF) recently computed *ab initio* by Sheehy et al.[9]

For the C-A system the ETMF was assumed to be the same as for the D-A system (justified since the potential energy curves of the C and D states are nearly identical, at least in the potential well for the first four or so vibrational levels with appreciable populations). The rotational levels of the NO $C^2\Pi$ state are perturbed due to interactions between this state and near resonant levels of the NO $D^2\Pi$ ($v \geq 0$) and $B^2\Pi$ ($v \geq 7$) states.[10,11] If these perturbations are neglected, the synthesized spectra fail to reproduce the measurements. This point is illustrated in Fig. 7 where, without an account of the perturbations, the position of the synthesized Q branch of the (C-A) 0-0 band is shifted by approximately 70 Å and its peak intensity is higher than the experiment by a factor 1.6. For this reason, perturbed rotational term energies for the (C, v=0) state were introduced in NEQAIR2-IR. They were computed using the 11×11 Hamiltonian and related spectroscopic constants (term energies, rotational constants, spin-splitting and Λ-doubling constants, and electronic interaction parameters) published by Amiot and Vergès.[11] The model is presently limited to rotational levels of (C, v=0) which is the only vibrational level analyzed by Amiot and Vergès. As the 0-0 band is responsible here for the dominant fraction (~55%) of the total (C-A) emission, significantly better agreement with experiment is already obtained (see Fig. 7). The remaining discrepancy in the range 1.18 to 1.21 μm may be eliminated when accurate measurements of rotational term energies and perturbations in higher vibrational levels of the C state are available (in particular for $v' = 1$ since the 1-1 band emits approximately 25% of the C-A total emission).

At relatively high pressures where inverse predissociation is important, the population of the predissociating NO C state is proportional to the populations of atomic oxygen and nitrogen.[4] As ground state atomic oxygen and nitrogen concentrations can therefore be measured from the intensity of the C-A transition, this system is of great interest for optical diagnostics.

In contrast with those of the C-A and D-A systems, the transition probabilities of the E-C, E-D, F-C, H-C, H′-C, H-D, and H′-D systems are not well established. Nevertheless, these systems are strongly diagonal (Franck-Condon factors for the $\Delta v = 0$ bands are typically greater than 0.95) and each $\Delta v = 0$ sequence spans a narrow range of wavelengths or internuclear distances. As a result, the electronic transition moment is approximately the same for all bands in a given $\Delta v = 0$ sequence. If the transition probability of one band of a given system is known, the transition probabilities of other bands of the same system can then be determined. The oscillator strengths measured by Wray[8] for the 0-0 or 1-1 bands of the F-C, H-C, H'-C, H-D, and H'-D systems were used

here to infer transition probabilities for the other, non-measured bands. Simulations based on these values were found to be consistent with the measurements, except for the F-C and H-C systems for which better agreement was obtained using oscillator strengths twice as large as those recommended by Wray[8] (see Figure 8).

For the E-D system, we are not aware of any prior measurement or calculation of the transition probability. Therefore, we estimated the transition probability of this (weak) system by direct comparison with the measured spectrum (Figure 9). The value is listed in Table 2 along with our transition probability estimates for the F-C and H-C systems.

The Meinel system of N_2^+ was included in NEQAIR2-IR with transition probabilities based on the accurate electronic transition moment function computed by Langhoff et al.[12] This system appears as a weak continuum-like structure in the range 0.8 - 2.5 μm.

As can be seen in Fig. 9, several features of the experimental spectrum between 1.3 and 1.5 μm were not reproduced by baseline NEQAIR2 simulations. Based on the work of Biémont and Grevesse,[13] most of these features could be identified as corresponding to atomic lines of nitrogen. After introduction of the wavelengths and Einstein A coefficients tabulated by Biémont and Grevesse[13] for these lines, very good agreement is obtained between experiment and simulations (Fig. 9).

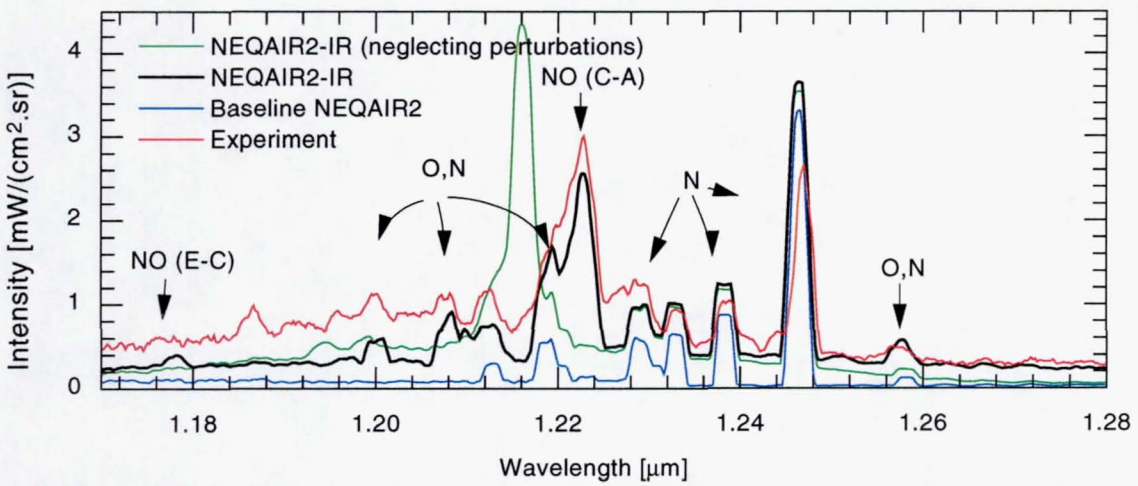

Figure 7. Measurements and simulations of the C-A system of NO. Note the large error in the model when perturbations are neglected.

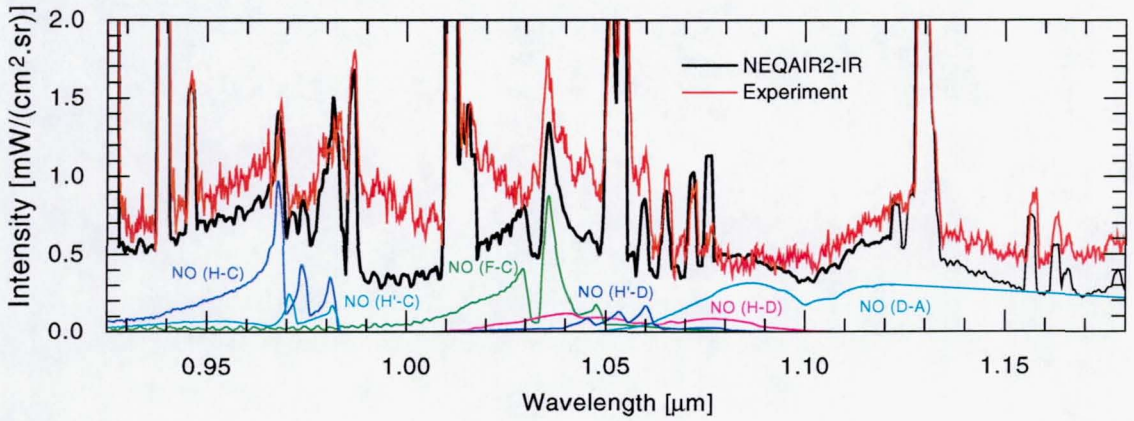

Figure 8. Measurements and simulations emphasizing the contributions of electronic transitions of NO.

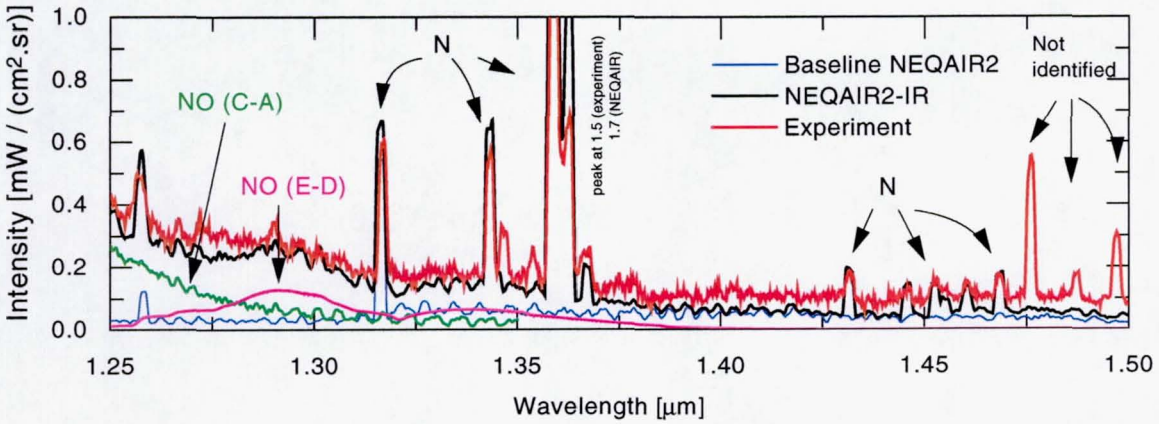

Figure 9. Measurements and simulations emphasizing the NO E-D system and the nitrogen lines added to NEQAIR2-IR.

2.4.2 Range 1.5–3.0 μm

The experimental spectra shown in Fig. 10 for the range 1.5-2.0 μm and in Fig. 11 for the range 2.0-3.0 μm exhibit numerous atomic lines and significant continuum radiation. Simulations with the baseline NEQAIR2 reproduce none of the lines and only a small fraction of the continuum radiation.

The lines are missing because the database of NEQAIR2, limited to the transitions listed by Wiese et al,[14] covers only the range 0.11-1.26 μm for atomic nitrogen and 0.08-1.32 μm for atomic oxygen. The database should be extended using the wavelengths and transition probabilities of Biémont and Grevesse[13] and Chung et al.[15]

The continuum radiation modeled in the baseline NEQAIR is limited to the free-bound recombination continua of atomic oxygen and nitrogen, and the free-free continuum (bremstrahlung radiation). Since the total predicted continuum radiation is much lower than experimentally observed, molecular continua or diffuse band systems could be missing in the code. The N_2^+ Meinel system was suspected initially, but its radiation (shown in Fig. 10 as the difference between the baseline NEQAIR2 and NEQAIR2-IR) is too weak to account for the missing continuum. Further work is required to resolve the discrepancy.

To determine the importance of absorption by the 5 meter-length of room air separating the plasma from the detector, the absorption coefficients of CO_2 and H_2O lines at 293 K were determined using the low-temperature radiation database HITRAN.[16] By comparing the emission and absorption spectra shown in Figs. 10 and 11, it can be seen that H_2O absorption is likely responsible for partial extinction of the signal around 1.82-1.92 μm and 2.55-2.8 μm. Outside these two narrow ranges, however, no absorption by room air can be detected.

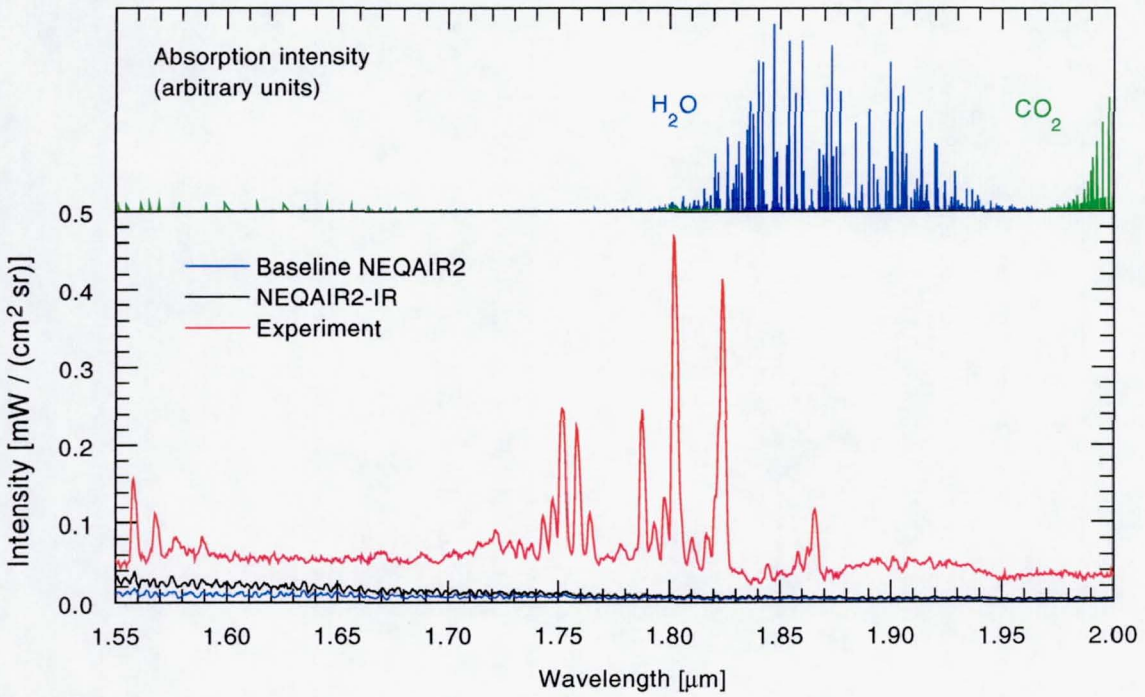

Figure 10. Bottom: Measurements and simulations between 1.55 and 2.0 μm. Top: Absorption spectra of H_2O and CO_2 at 273 K.

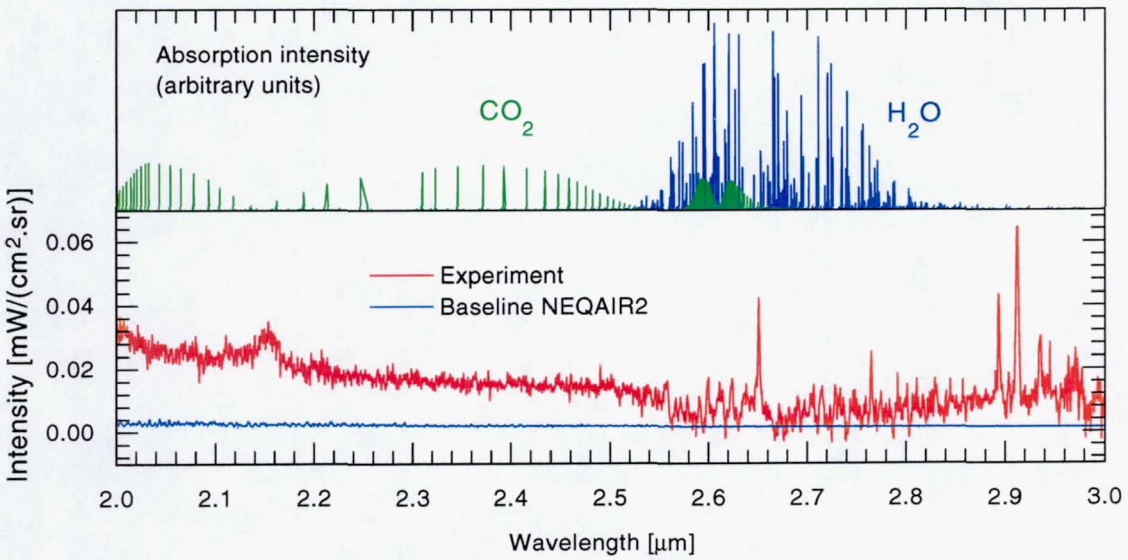

Figure 11. Bottom: Measurements and simulations between 2.0 and 3.0 μm. Top: Absorption spectra of H_2O and CO_2 at 273 K.

2.4.3 Range 3.0–4.8 μm

The experimental spectrum shown in Fig. 12 again exhibits numerous features that the baseline NEQAIR2 model, limited to the free-bound and free-free continua of atomic oxygen and nitrogen, does not predict.

Numerous atomic lines, including 140 oxygen and 108 nitrogen lines, were incorporated in NEQAIR2-IR. These lines were extracted from Ref. 13 (for the most part) and from Refs. 15, 17, 18 and 19. They originate from upper levels between 4p ^{4}S and 6d ^{4}F in the case of nitrogen, and between 4s ^{3}D and 20d ^{3}D in the case of oxygen. With this extended database, NEQAIR2-IR reproduces most of the atomic lines observed in the experiment. The predicted and measured intensities agree within a factor 2. Yet, there still remain unmodeled atomic lines, particularly around 4 μm (see Fig. 12).

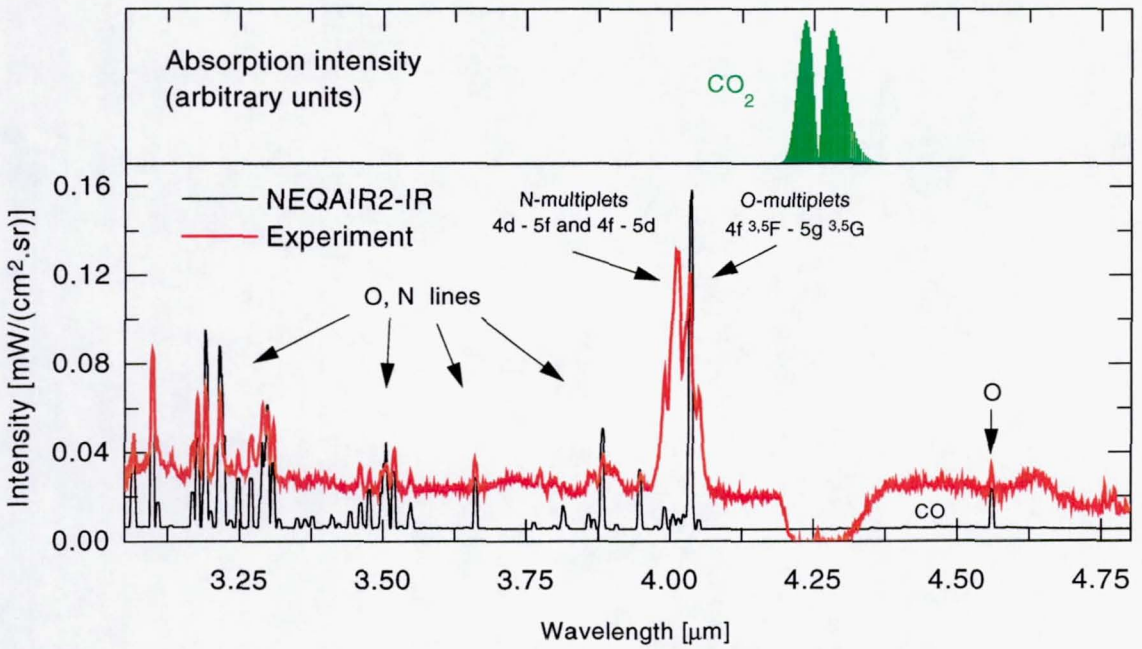

Figure 12. Bottom: Measurements and simulations between 3.0 and 4.8 μm. Top: Absorption spectrum of CO_2 at 273 K.

Saum and Benesch[18,19] identified several lines around 4 μm as belonging to the 4f–5g multiplet of oxygen and the 4d–5f and 4f–5d of nitrogen. These transitions are likely to be the features observed around 4 μm. To introduce them into NEQAIR2-IR, upper state term energies, wavelengths, and Einstein A coefficients were required. The energies of the terms ^{5}G, ^{3}G of the 5g state of oxygen are not listed in the wavelength tables of Moore[20] as these levels lie above the highest state in the tables. Nevertheless, term energies for these states were determined by Chang et al[21] and Einstein A coefficients were calculated by Chung et al.[15] For the nitrogen systems, the line positions were

obtained from the tables of Moore,[20] but no Einstein A coefficients could be found in the literature. These lines were entered in NEQAIR2-IR with arbitrary (small) Einstein A coefficients. As can be seen in Fig. 12, wherein they appear between 3.991 and 4.035 μm, these lines are likely to be the features observed around 4 μm.

The HITRAN database[16] was used to determine room air absorption. As can be seen in Fig. 12, the strong absorption band of CO_2 at ~4.25 μm is responsible for almost total extinction of the plasma spectrum in the corresponding wavelength range. This shows that the continuum observed in the measured spectrum is not an experimental artifact. More work is needed to better understand and model this continuum as it is not well predicted by the free-bound and free-free continua included in the baseline NEQAIR2.

As the air injected in the torch contained some CO_2 (approximately 330 parts/million), it was thought that CO could emit significant radiation via its vibrational-rotational spectrum around 4.4 μm. This system was therefore implemented in NEQAIR2-IR using the *ab initio* dipole moment function of Langhoff and Bauschlicher[22] and line positions based on the spectroscopic constants of Huber and Herzberg.[23] As can be seen in Fig. 12, however, the contribution of this system was found to be negligible.

2.4.4 Range 4.8–5.5 μm: NO Fundamental

The fundamental ($\Delta v = 1$) rovibrational transitions of ground state NO ($X^2\Pi$) are clearly seen in the experimental spectrum shown in Fig. 13. A detailed, accurate model for the fundamental bands (and overtones) of NO ($X^2\Pi$) was implemented in NEQAIR2-IR. The model calculates rotational line positions by diagonalizing the Hamiltonian published by Amiot.[24] Line intensities are computed similarly to those of $^2\Pi$-$^2\Pi$ electronic transitions, except that the electronic-vibrational transition moment is replaced with the vibrational dipole moment, $M_{v'v''}$, defined as:

$$\left(M_{v'v''}\right)^2 = \left(\int \Psi_{v'}(r) D_e(r) \Psi_{v'}(r) dr\right)^2, \qquad (3)$$

where D_e stands for the electric dipole moment function (EDMF). Values of the vibrational dipole moment were determined using the accurate *ab initio* EDMF recently computed by Langhoff et al.[25] Finally, the Hönl-London factor expressions recommended by Spencer et al.[26] were employed. The model provides very accurate line intensities and spectral positions which is of particular importance for high-resolution spectroscopic diagnostics and for accurate simulations of the absorption by H_2O.

The HITRAN database[16] was used to determine the transmittance spectrum of room air (based on a water partial pressure of ~7.5 torr). This spectrum, plotted in Figure 13,

emphasizes the effect of absorption by water along the 5 m optical train. This absorption was taken into account in the NEQAIR2-IR simulations shown in Fig. 13 as well.

The line-of-sight spectral simulations adopted the measured radial temperature profile which, as seen in Fig. 4, excludes the outer 0.5 cm-wide portion of the plasma. Accordingly, these simulations only account for regions of the plasma at temperatures between 7900 and ~5500 K Yet, as the equilibrium mole fraction of NO is much larger at lower temperatures, with a maximum at ~3400 K, the edges of the plasma between 2 and 2.5 cm are likely to be source of most NO fundamental emission. It is therefore not surprising that simulations based on the temperature profile of Fig. 4 underestimate the NO fundamental. In fact, as can be seen in Fig. 13, better agreement with the measurements is already obtained by simply extrapolating the temperature profile of Fig. 4 to a radius of 2.5 cm. Further measurements of temperature and NO concentration at the edges of the plasma would be needed to fully resolve this issue.

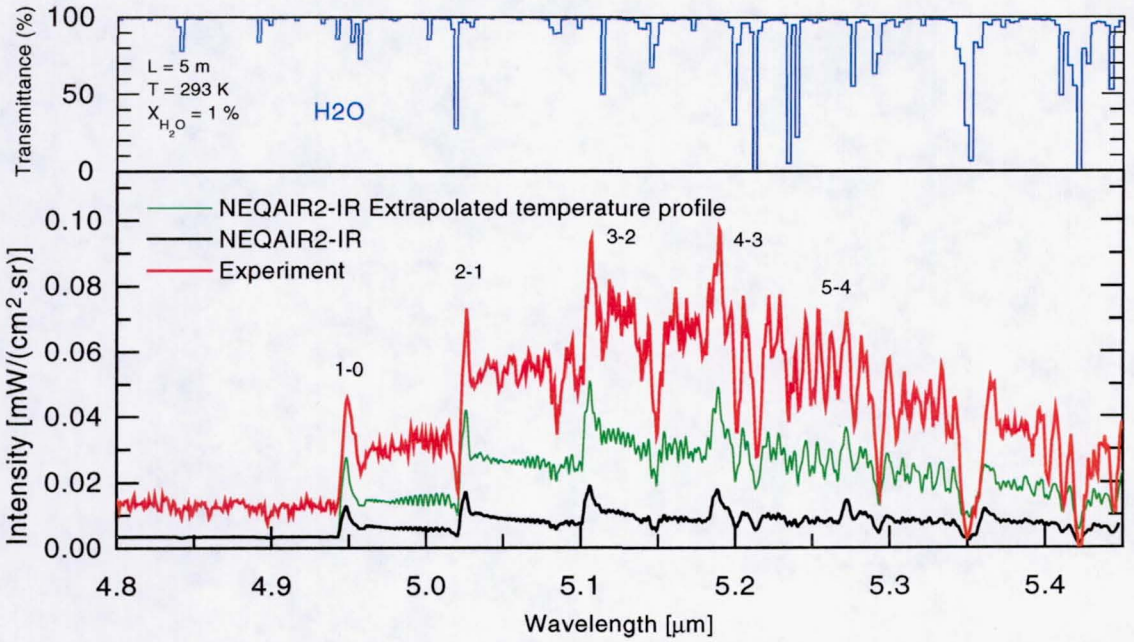

Figure 13. Bottom: Measurements and simulations between 4.8 and 5.5 μm.
Top: Spectral transmittance of a 5-m length of air at 273 K
with p_{H2O} = 7.5 torr.

2.5 Conclusion

The radiative emission of high-temperature air (~7900 K) at conditions close to local thermodynamic equilibrium was measured in the infrared spectral range between 0.8 and 5.5 μm. The measured spectra were corrected for the spectral response of the detection system and calibrated in intensity. These benchmark spectra were then used to guide the extension of the NEQAIR radiation code up to 5.5 μm. The molecular and atomic transitions listed in Table 3 were incorporated into an extended model called NEQAIR2-IR.

The major spectral features observed between 0.8 and 1.5 μm are atomic lines of N and O and electronic transitions between high-lying Rydberg states of NO. The atomic radiation database of NEQAIR2, originally limited to the transitions listed in the tables of Wiese et al[14] which all lie below ~1.2 μm, was extended to the range 1.2-1.5 μm based on the work of Biemont and Grevesse.[13] Most atomic lines are now reproduced with good accuracy by NEQAIR2-IR in this range Eight electronic NO transitions were also introduced into NEQAIR2-IR. Although the model would clearly benefit from accurate measurements of rotational term energies in the C ($v' \geq 1$), E, F, H and H' states of NO, reasonable agreement is obtained with the measurements.

The radiation observed between 1.5 and 4.8 μm appears to be due for the most part to atomic lines and to an underlying, unidentified continuum. The baseline NEQAIR2 model does not include any of the lines, and predicts a continuum intensity much weaker than in the measurements. The addition of atomic transitions to the radiation database in the range 3-4.8 μm was comprehensive, yet there still remain unmodeled atomic lines. These lines are likely due to transitions from high-lying nitrogen and oxygen states for which Einstein-A coefficients and accurate wavelengths remain to be determined. The Meinel system of N_2^+ was added to NEQAIR2-IR and found to be responsible for a small fraction of the observed continuum. The CO vibrational-rotational bands, on the other hand, were found to have a negligible radiative contribution. The unexplained remaining portion of the continuum could be due to molecular free-bound continua or to diffuse molecular transitions (O_2 atmospheric system, N_2 Mac Farlane system[23]). More work is required to understand the origin of the observed continuum and to improve its modeling.

Finally, the fundamental bands of the vibration-rotation spectrum of NO were observed in the experiment (between 4.8 and 5.5 μm). An accurate model was added to NEQAIR2-IR for this transition (fundamental and overtones). This model can be used in future work for temperature and NO concentration measurements.

Table 3. Infrared transitions modeled in the baseline NEQAIR and in the NEQAIR2-IR code developed in the context of this research grant.

Species	Baseline NEQAIR	New NEQAIR2-IR
O, N	no line above 1.3 μm	360 new lines
N_2^+		$A\ ^2\Pi - X\ ^2\Sigma^+$ (Meinel system)
NO		$C\ ^2\Pi - A\ ^2\Sigma^+$
		$D\ ^2\Sigma^+ - A\ ^2\Sigma^+$
		$E\ ^2\Sigma^+ - C\ ^2\Pi$
		$E\ ^2\Sigma^+ - D\ ^2\Sigma^+$
		$F\ ^2\Delta - C\ ^2\Pi$
		$H\ ^2\Sigma^+ - C\ ^2\Pi$
		$H'\ ^2\Pi - C\ ^2\Pi$
		$H\ ^2\Sigma^+ - D\ ^2\Sigma^+$
		$H'\ ^2\Pi - D\ ^2\Sigma^+$
NO		$X\ ^2\Pi - X\ ^2\Pi$ (Vibration-Rotation)
CO		$X\ ^1\Sigma^+ - X\ ^1\Sigma^+$ (Vibration-Rotation)

3. References

1. Goody, R.M., *Atmospheric Radiation. I. Theoretical basis*, Oxford University Press, Amen House, London, p. 4, 1964.
2. Wolfe, W.L. and Zissis, G.J., *The Infrared Radiation Handbook*, pp. 5-87, Office of Naval Research, Department of the Navy, Washington, D.C., 1978.
3. Park, C., "Nonequilibrium Air Radiation (NEQAIR) Program: User's Manual," *NASA TM 86707*, Ames Research Center, Moffett Field, CA 94035, 1985.
4. Laux, C.O., Gessman, R.J., and Kruger, C.H., "Modeling the UV and VUV Radiative Emission of High-Temperature Air," *AIAA Paper 93-2802*, AIAA 28th Thermophysics Conference, Orlando, FL, July 6-9 1993.
5. Laux, C.O., "Optical Diagnostics and Radiative Emission of Air Plasmas," Ph.D. Thesis, *HTGL Report T-288*, Stanford University, August 1993.
6. Laux, C.O., Moreau, S., and Kruger, C.H., "Experimental Study and Improved Modeling of High-Temperature Air Radiation," *AIAA 92-2969*, AIAA 23rd Plasmadynamics and Lasers Conference, Nashville, TN, July 6-8, 1992.
7. Moreau, S., Laux, C.O., Chapman, D.R, and MacCormack, R.W., "A More Accurate Non-Equilibrium Air Radiation Code: NEQAIR Second Generation," *AIAA-2968*, AIAA 23rd Plasmadynamics and Lasers Conference, Nashville, TN, July 6-8, 1992.
8. Wray, K.L., "Oscillator Strengths of Transitions between Rydberg States of Nitric Oxide in the Near IR," *JQSRT*, Vol. 9, pp. 255-276, 1969.

9. Sheehy, J.A., Bauschlicher, C.W., Jr., Langhoff, S.R., and Partridge, H., "Theoretical Study of the Nitric Oxide ε and 11 000 Å Bands," *Chem. Phys. Letters*, Vol. 225, pp. 221-228, 1994.

10. Lagerqvist, A. and Miescher, E., "Absorptions spektrum des NO-Moleküls Feinstruktur-Analyse der δ- und β-Banden und Homogene Störung $C^2\Pi$–$B^2\Pi$," *Helv. Phys. Acta*, Vol. 31, pp. 221-262, 1958.

11. Amiot, C. and Vergès, J., "Fine Structure of the $C^2\Pi$–$A^2\Sigma^+$ and $D^2\Sigma^+$–$A^2\Sigma^+$ Band Systems of the NO Molecule: Homogeneous and Heterogeneous Perturbations," *Phys. Scripta*, Vol. 25., pp. 302-311, 1982.

12. Langhoff, S.R. and Bauschlicher, C.W., Jr., "Theoretical Study of the First and Second Negative Systems of N_2^+," *J. Chem. Phys.*, Vol. 94, p. 6638, 1991.

13. Biémont, E. and Grevesse, N., "Infrared Wavelengths and Transition Probabilities for Atoms, $3 \leq Z \leq 20$," *Atomic Data and Nuclear Data Tables*, Vol. 12, pp. 217-310, 1973.

14. Wiese, W.L., Smith, M.W., and Glennon B.M., *Atomic Transition Probabilities*, National Standard Reference Data Series, National Bureau of Standards, 4, 1966.

15. Chung, S., Lin, C.C., and Lee, E.T.P., "Transition Probabilities of O I Spectral Lines," *JQSRT*, Vol. 36, pp.19-37, 1986.

16. Rothman, L.S., Gamache, R.R., Goldman, A., Brown, L.R., Toth, R.A., Pickett, H.M., Poynter, R.L., Flaud, J.-M., Camy-Peyret, C., Barbe, A., Husson, N., Rinsland, C.P., and Smith, M.A.H., "The HITRAN Database: 1986 Edition," *Appl. Optics*, Vol. 26, pp. 4058-ff, 1987.

17. Hibbert, A., Biémont, E., Godefroid, M., and Vaeck, N., "Accurate Transition Probabilities for Astrophysically Important Spectral Lines of Neutral Nitrogen," *Astrophys. Suppl. Ser.*, Vol. 88, pp.505-524, 1991.

18. Saum, K.A. and Benesch, W.M, "Infrared Electronic Emission Spectrum of Nitrogen," *Appl. Optics*, Vol.9, pp. 195-200, 1970.

19. Saum, K.A. and Benesch, W.M, "Infrared Electronic Emission Spectrum of Oxygen," *Appl. Optics*, Vol.9, pp. 1419-1423, 1970.

20. Moore, C.E., "Selected Tables of Atomic Spectra," *NSRDS-NBS* 3, Sec. 5, U.S. Government Printing Office, Washington, D.C., 1975.

21. Chang, E.S., Barowy, W.M., and Sakai, H., "Non-Penetrating States of Atomic Oxygen," *Physica Scripta*, Vol. 38, pp. 1987.

22. Langhoff, S.R. and Bauschlicher, C.W., Jr., "Global Dipole Moment Function for the $X^1\Sigma^+$ Ground State of CO,"*J. Chem. Phys.*, Vol. 102, 5220, 1995.

23. Huber, K.P. and Herzberg, G., *Molecular spectra and Molecular structure. IV. Constants of diatomic molecules*, Van-Nostrand-Reinhold, New York, 1979.

24. Amiot, C., "The Infrared Emission of NO : Analysis of the $\Delta v = 3$ Sequence up to $v = 22$", *J. Molec. Spectrosc.*, Vol. 94, pp. 150-172, 1982.

25. Langhoff, S.R., Bauschlicher, C.W., Jr., and Partridge, H., "Theoretical Dipole Moment for the $X^2\Pi$ state of NO," *Chem. Phys. Letters,* Vol. 223, pp. 416-422, 1994.

26. Spencer, M.N., Chackerian, C., Jr., and Giver, L.P., "The Nitric Oxide Fundamental Band: Frequency and Shape Parameters for Rovibrational Lines," *J. Molec. Spectrosc.*, Vol. 165, pp. 506-524, 1994.

4. Publications and Presentations

Laux, C.O., Gessman, R.J., Hilbert, B., and Kruger C.H., "Radiative and Kinetic Studies of Nonequilibrium Air and Nitrogen Plasmas," Missile Signatures and Aerothermochemistry Meeting, NASA-Ames Research Center, Moffett Field, CA, April 22-23, 1996.

Laux, C.O., Gessman, R.J., Hilbert, B. and Kruger, C.H., "Experimental Study and Modeling of Infrared Air Plasma Radiation," AIAA 95-2124, 30th AIAA Thermophysics Conference, San Diego, CA, June 19-22, 1995.

Laux, C.O., Gessman, R.J., and Kruger, C.H., "Experimental Studies and Theoretical Modeling of Air Plasmas Produced in an ICP Torch," Missile Signatures and Aerothermochemistry Meeting, Space Dynamics Laboratory, Utah State University, Logan, UT, April 7, 1994.

5. Personnel

The following personnel contributed to this research:

Prof. Charles H. Kruger	Vice-Provost, Dean of Research and Graduate Policy, Professor, Department of Mechanical Engineering.
Dr. Christophe O. Laux	Research Associate High Temperature Gasdynamics Laboratory, Department of Mechanical Engineering. (Ph.D. Mechanical Engineering, Stanford University 1993).
Richard J. Gessman	Graduate Research Assistant, High Temperature Gasdynamics Laboratory, Department of Mechanical Engineering. (M.S. Aeronautical and Aerospace Engineering, University of Illinois at Champaign-Urbana, 1992).
Benoit Hilbert	Graduate Research Assistant, High Temperature Gasdynamics Laboratory, Department of Mechanical Engineering. (M.S. Mechanical Engineering, Stanford University, 1995).
Denis Packan	Graduate Research Assistant, High Temperature Gasdynamics Laboratory, Department of Mechanical Engineering. (M.S. Engineering, Ecole Centrale Paris, 1996).